

Research Journal of Pharmaceutical, Biological and Chemical Sciences

Monte Carlo Simulation and Electrochemical Assessment of Inhibitive Behavior of Pyrazole Derivative On Mild Steel in HCl Medium.

Toumiat K¹, EL Aoufir Y^{2,3}, Lgaz H^{2,4}, Salghi R^{4*}, Jodeh S⁵, Zougagh M^{6,7}, and Oudda H².

¹Department of Materials Sciences, Laghouat University, PO Box 37, 03000, Laghouat, Algeria.

²Laboratory of separation methods, Faculty of Science, Ibn Tofail University PO Box 242, Kenitra, Morocco.

³Laboratoire des matériaux, nanotechnologie et environnement. Université M^{ed}V, Rabat, Morocco.

⁴Laboratory of Applied Chemistry and Environment, ENSA, Ibn Zohr University, PO Box 1136, 80000 Agadir, Morocco.

⁵Department of Chemistry, An-Najah National University, P. O. Box 7, Nablus, Palestine.

⁶Regional Institute for Applied Chemistry Research, IRICA, Ciudad Real, Spain.

⁷Albacete Science and Technology Park, E-02006, Albacete, Spain.

ABSTRACT

Inhibitive performance of pyrazole derivative namely, 3,5-Diphenylpyrazole (DPP) on corrosion behavior of mild steel in 1.0 M HCl solution was investigated by means of electrochemical techniques, weight loss and Monte Carlo simulation. The increase in concentration shows a positive effect on inhibition efficiency. Inhibitor molecules directly adsorb at surface based on donor–acceptor interactions between the π -electrons of benzene, and nitrogen atoms and the vacant d-orbitals of iron atoms. According to the thermodynamic parameters, present inhibitor adsorb physicochemical. The potentiodynamic polarization shows that the pyrazole derivative is mixed type in nature. In this article, Monte Carlo simulation searches of the configurational space of iron (1 1 0) (substrate) – DPP (adsorbate) system to find low energy adsorption sites on both adsorbate and substrate system. The results indicated that DPP could adsorb on Fe surface through the nitrogen atoms and benzenes rings in its molecule.

Keywords: Corrosion inhibition, Mild steel, EIS, 3,5-Diphenylpyrazole, Monte Carlo

**Corresponding author*

INTRODUCTION

Mild steel is widely applied as constructional material in many industries due to its excellent mechanical properties and low cost. Some of the important fields of applications of mild steel are acid pickling in hydrochloric acid (HCl), industrial cleaning, acid descaling, oil-well acidizing and petrochemical processes, however the main problem of applying mild steel is its dissolution in acidic solutions[1–4]. Several methods are available for corrosion prevention. Employing inhibitors is one of the cost-effective protection methods of metals and alloys in acids such as hydrochloric acid[5–7]. Generally, Inhibitors are organic components, which have nitrogen, oxygen and sulfur in their molecular. The inhibiting effect is generally explained by the formation of a physical and/or chemical adsorption film barrier on the metal surface[8–13]. Physisorption involves electrostatic forces between ionic charges or dipoles on the adsorbed species and the electric charge at metal/solution interface. Chemisorption, involves charge sharing or charge transfer from the inhibitor molecules to the metal surface to form a coordinate type bond[14–19]. In fact, electron transfer is normally proposed for transition metals having vacant low-energy electron orbital. Chemisorption is characterized by stronger adsorption energy than physical adsorption[20–27]. The pyrazole family has nitrogen in their molecular structure and heterocyclic group, which can create the inhibition properties in acidic media and can be adsorbed onto the surface.

In this work, the adsorption behavior of pyrazole derivative (3,5-Diphenylpyrazole (DPP)) at Fe surface will investigated by weight loss, electrochemical and the Monte Carlo simulation method. The inhibitor molecule used in this paper was purchased from Sigma–Aldrich and have the structure presented in Fig. 1. As can be seen, they have different active groups, which can act as adsorption centers.

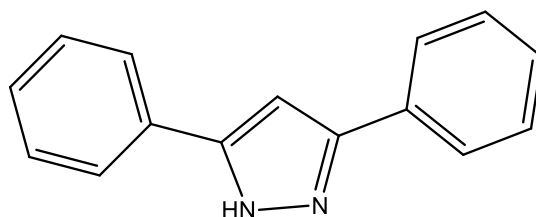


Figure 1. Chemical structure of inhibitor.

MATERIALS AND METHODS

Chemicals and Gravimetric measurements

Corrosion tests have been performed, using the gravimetric and electrochemical measurements, on electrodes cut from sheets of carbon steel with the chemical composition: 0.370 % C, 0.230 % Si, 0.680 % Mn, 0.016 % S, 0.077 % Cr, 0.011 % Ti, 0.059 % Ni, 0.009 % Co, 0.160 % Cu, and the remainder iron.

The aggressive medium of molar hydrochloric acid used for all studies were prepared by dilution of analytical grade 37% HCl with double distilled water. The concentrations of DPP used in this investigates were varied from 1.10^{-4} to 5.10^{-3} M.

Gravimetric measurements were realized in a double walled glass cell equipped with a thermostat-cooling condenser. The carbon steel specimens used have a rectangular form with dimension of $2.5 \times 2.0 \times 0.2$ cm were abraded with a different grade of emery paper (320-800-1200) and then washed thoroughly with distilled water and acetone. After weighing accurately, the specimens were immersed in beakers, which contained 100 ml acid solutions without and with various concentrations of DPP at temperature equal to 303 K remained by a water thermostat for 6h as immersion time. The gravimetric tests were performed by triplicate at same conditions.

The corrosion rates (C_R) and the inhibition efficiency ($\eta_{wt} \%$) of carbon steel have been evaluated from mass loss measurement using the following equations:

$$C_R = \frac{w}{St} \quad (1)$$

$$\eta_{wt} \% = \frac{C_R^0 - C_R}{C_R^0} \times 100 \quad (2)$$

Where w is the average weight loss before and after exposure, respectively, S is the surface area of sample, t is the exposure time, C_R^0 and C_R is the corrosion rates of steel without and with the DPP inhibitor, respectively.

Electrochemical tests

The potentiodynamic polarization curves were conducted using an electrochemical measurement system PGZ 100 Potentiostat/Galvanostat controlled by a PC supported by the Voltmaster 4.0 Software. The electrochemical measurements were performed in a conventional three electrode glass cell with carbon steel as a working electrode, platinum as counter electrode (Pt) and a saturated calomel electrode used as a reference electrode. The working electrode surface was prepared as described above gravimetric section. Prior to each electrochemical test an immersion time of 30 min was given to allow the stabilization system at corrosion potential. The polarization curves were obtained by changing the electrode potential automatically from -800 to -200 mV/SCE at a scan rate of 1 mV s⁻¹. The temperature is thermostatically controlled at desired temperature ± 1 K. The percentage protection efficiency (η_p %) is defined as:

$$\eta_{PDP} (\%) = \frac{i_{CORR}^0 - i_{CORR}}{i_{CORR}^0} \times 100 \quad (3)$$

Where, i_{CORR}^0 are corrosion current in the absence of inhibitor, i_{CORR} are corrosion current in the presence of inhibitor.

Electrochemical impedance spectroscopy (EIS) measurements were carried out with same equipment used for potentiodynamic polarization study (Voltalab PGZ 100) at applied sinusoidal potential waves of 5mV amplitudes with frequencies ranging from 100 KHz to 10 mHz at corrosion potential. The impedance diagrams are given in the Nyquist representation. The charge transfer resistance (R_{ct}) was determined from Nyquist plots and double layer capacitance (C_{dl}) was calculated from CPE parameters of the equivalent circuit deduced using Zview software. In this case the percentage protection efficiency (η_{EIS} %) is can be calculated by the value of the charge transfer resistance (R_{ct})

$$\eta_{EIS} (\%) = \frac{R_{ct} - R_{ct}^0}{R_{ct}} \times 100 \quad (4)$$

Where R_{ct}^0 and R_{ct} were the polarization resistance of uninhibited and inhibited solutions, respectively.

Monte Carlo simulation study

The Monte Carlo (MC) search was adopted to compute the low configuration adsorption energy of the interactions of the DPP on a clean iron surface. The Monte Carlo (MC) simulation was carried out using Materials Studio 6.0 software (Accelrys, Inc.) [28]. The Fe crystal was cleaved along the (110) plane, it is the most stable surface as reported in the literature. Then, the Fe (110) plane was enlarged to (8x8) supercell to provide a large surface for the interaction of the inhibitor. The simulation of the interaction between DPP and the Fe (110) surface was carried out in a simulation box (19.85 × 19.85 × 38.10 Å) with periodic boundary conditions, which modeled a representative part of the interface devoid of any arbitrary boundary effects. After that, a vacuum slab with 30 Å thickness was built above the Fe (110) plane. All simulations were implemented with the COMPASS force field to optimize the structures of all components of the system of interest. More simulation details on the methodology of Monte Carlo simulations can be found in previous publications [29–31]

RESULTS AND DISCUSSION

Weight loss study

Values of the inhibition efficiency and corrosion rate obtained from the weight loss measurements of carbon steel for different concentrations of inhibitor in 1 M HCl at 303 K after 6 h of immersion are given in Table 1. This shows that the inhibition efficiency increases with the increasing inhibitor concentration. At this purpose, one observes that the optimum concentration of inhibitor required to achieve the efficiency is found to be 5×10^{-3} M ($\eta\% = 93.62\%$). The inhibition of corrosion of mild steel by DPP can be explained in terms of adsorption on the metal surface. This compound can be adsorbed on the metal surface by the interaction between lone pairs of electrons of nitrogen atoms and benzenes rings of the inhibitor and the metal surface. This process is facilitated by the presence of vacant orbitals of low energy in iron atom, as observed in the transition group metals[19].

Table 1: Inhibition efficiency of various concentrations of DPP for corrosion of MS in 1M HCl obtained by weight loss measurements at 303K.

Inhibitors	Concentration (mM)	C_R ($\text{mg cm}^{-2} \text{h}^{-1}$)	η_w (%)	θ
Blank	1.0	1.135	-	-
DPP	5.10^{-3}	0.0724	93.62	0.9362
	1.10^{-3}	0.0922	91.87	0.9187
	5.10^{-4}	0.1308	88.47	0.8847
	1.10^{-4}	0.1598	85.92	0.8592

PDP results

Fig. 2 shows polarization curves for mild steel in 1.0 M HCl at 303 K after 0.5 h immersion at various concentrations of DPP. Electrochemical parameters which could be extracted from polarization curves such as corrosion potential (E_{corr}), corrosion current density (i_{corr}), cathodic Tafel slope (β_c) are measured by Tafel extrapolation and presented in Table 2. In addition, considering the corrosion current densities i_{corr} in absence and presence of inhibitor, values of surface coverage (θ) and inhibitor efficiency ($IE\%$) is calculated by mentioned equation in experimental part. The DPP decreased the anodic current, which is related with dissolution of mild steel. The addition of DPP to acid solutions shifts also the cathodic branches to lower values of current density at all investigated concentrations. This result indicated that DPP exhibited cathodic and anodic inhibition effects. Therefore, DPP can be classified as inhibitor of relatively mixed effect in 1 M HCl[14,15].

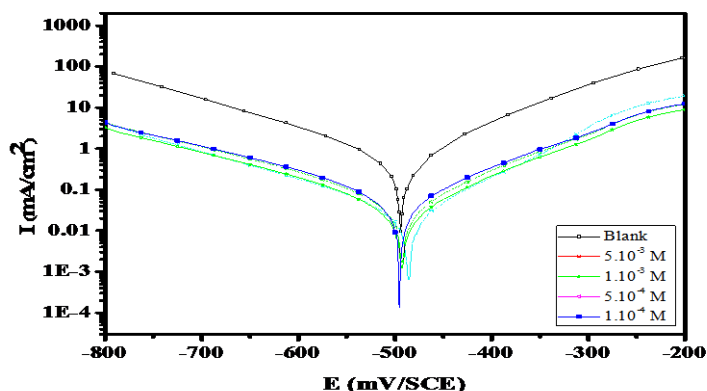


Figure 2. Polarisation curves of MS in 1 M HCl for various concentrations of DPP at 303K.

It can be seen from the polarization results presented in Table 2 that the corrosion current density decreased noticeably with the increase in inhibitor concentration. The corrosion potential of mild steel shifted slightly compared to the blank, confirming that the DPP control the cathodic and anodic reactions, although

there was not a specific relation between E_{corr} and inhibitor concentrations. The values of IE (%) increases noticeably with the increase in DPP concentrations.

Table 2. Corrosion parameters for corrosion of MS with selected concentrations of DPP in 1 M HCl by Potentiodynamic polarization method at 303K.

Inhibitor	Concentration (M)	$-E_{corr}$ (mV/SCE)	$-\beta_c$ (mV dec ⁻¹)	i_{corr} ($\mu\text{A cm}^{-2}$)	η_{Tafel} (%)	Θ
Blank	-	496	162.0	564.0	-	-
DPP	5.10^{-3}	488.2	152.9	33.1	94.13	0.9413
	1.10^{-3}	494.2	167.2	47.1	91.64	0.9164
	5.10^{-4}	596.4	167.1	63.7	88.71	0.8871
	1.10^{-4}	498.7	174.5	78.4	86.10	0.8610

Electrochemical impedance spectroscopy (EIS)

The *EIS* measurements were achieved to determine important impedance parameters of the metal/solution interface in presence and absence of the inhibitor. Fig. 3 shows Nyquist plots for mild steel in 1 M HCl containing different concentrations of the DPP. The plots reveal depressed semicircle with a size dependent on the inhibitor concentration. It is obvious that the semicircle size increases with the inhibitor concentration indicating an increase in the charge transfer resistance of the metal/solution interface and then it had an inhibiting effect on steel corrosion in electrolyte solutions. When the complex plane impedance contains a “depressed” semicircle with the center under the real axis, such behavior characteristic for solid electrodes and often referred to as frequency dispersion have been attributed to roughness and inhomogeneities of the solid surfaces[17,18]. The impedance spectra were fitted to the $R_s(R_{ct}CPE)$ equivalent circuit of the form in Fig. 4. Where R_s is the solution resistance, R_{ct} denotes the charge-transfer resistance and *CPE* is constant phase element. The introduction of *CPE* into the circuit was necessitated to explain the depression of the capacitance semicircle, which corresponds to surface heterogeneity resulting from surface roughness, impurities, and adsorption of inhibitors[1]. The impedance of this element is frequency-dependent and can be calculated using the Eq. 5[10,11]:

$$Z_{CPE} = \frac{1}{Q(j\omega)^n} \tag{5}$$

Where Q is the *CPE* constant (in $\Omega^{-1} \text{S}^n \text{cm}^{-2}$), ω is the angular frequency (in rad s^{-1}), $j^2 = -1$ is the imaginary number and n is a *CPE* exponent which can be used as a gauge for the heterogeneity or roughness of the surface. In addition, the double layer capacitances, C_{dl} , for a circuit including a *CPE* were calculated by using the following Eq. 6:

$$C_{dl} = (Q \cdot R_{ct}^{1-n})^{1/n} \tag{6}$$

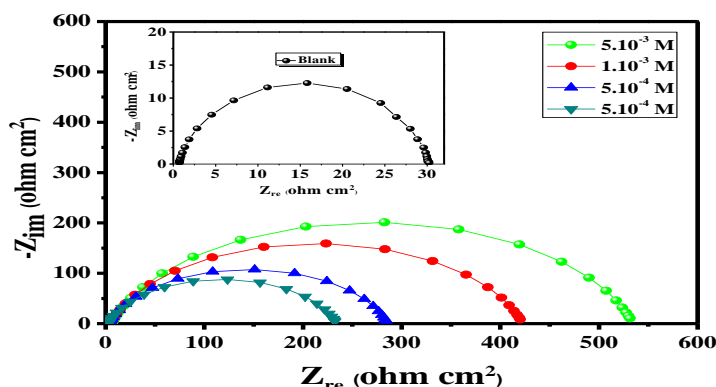


Figure 3. Nyquist curves for mild steel in 1 M HCl for selected concentrations of DPP at 303K.

Table 3. AC-impedance parameters for corrosion of mild steel for selected concentrations of DPP in 1M HCl at 303K.

Inhibitor	Concentration (M)	R_{ct} ($\Omega \text{ cm}^2$)	n	$Q \times 10^{-4}$ ($\text{s}^n \Omega^{-1} \text{ cm}^{-2}$)	C_{dl} ($\mu\text{F cm}^{-2}$)	η_{EIS} (%)	θ
Blank	1.0	29.35	0.910	1.7610	91.6	-	-
DPP	5.10^{-3}	528.5	0.829	0.1798	6.88	94.44	0.9444
	1.10^{-3}	417.9	0.832	0.2987	12.32	92.97	0.9297
	5.10^{-4}	282.7	0.865	0.3476	16.89	89.62	0.8962
	1.10^{-4}	231.1	0.894	0.5978	35.98	87.30	0.8730

Inspection of data in Table 3 shows clearly that R_{ct} and C_{dl} values have opposite trend at the whole concentration range (R_{ct} increases and C_{dl} decreases with inhibitor concentration). The decrease in this capacity with increase in inhibitor concentrations may be attributed to the formation of a protective layer on the electrode surface[20,21]. In addition, the value of the proportional factor Q of CPE varies in a regular manner with inhibitor concentration. It can be supposed that a protective layer covers the mild steel surface. The values of n lies between 0.829 and 0.894 in the case of inhibited solutions. Addition of pyrazole derivative decreases n values indicating reduction of surface inhomogeneity due to the adsorption of inhibitor molecules on the most active adsorption sites at the mild steel surface[32,33]. It is also obvious from the results that the DPP inhibit the corrosion of steel in 1 M HCl solution at all concentrations used in this study and the IE (%) was seen to increase continuously with increasing additive concentration at 303 K. Indeed, the maximum of IE (%) was achieved at 5.10^{-3} M of DPP. The inhibition efficiencies, calculated from ac impedance study, show the same trend as those obtained from polarization curves measurements and weight loss.


Figure 4. Equivalent electrical circuit corresponding to the corrosion process on the carbon steel in hydrochloric acid.

Adsorption isotherm

Adsorption of organic inhibitor on metal surface is always accompanied by replacement of water molecules adsorbed on the metal surface with organic molecules[34]. The values of surface coverage, θ corresponding to some extent of the inhibitor adsorption are derived from weight loss tests. The data of the surface coverage were found to fit with Langmuir isotherm which is given by[35]:

$$\frac{C}{\theta} = \frac{1}{K_{ads}} + C \quad (7)$$

Where, C is the concentration of the inhibitor, K_{ads} is the equilibrium constant of adsorption and θ is the surface coverage. The Langmuir approach is based on a molecular kinetic model of the adsorption-desorption process. On the other hand, the adsorption equilibrium constant (K_{ads}) is related to the standard free energy of adsorption (ΔG°_{ads}) of the inhibitor molecules by the following Eq. 8[22]:

$$K_{ads} = \frac{1}{55.5} \exp\left(\frac{-\Delta G^{\circ}_{ads}}{RT}\right) \quad (8)$$

Where R is the universal gas constant, T the absolute temperature in K, and 55.5 represents the molar concentration of water in the solution.

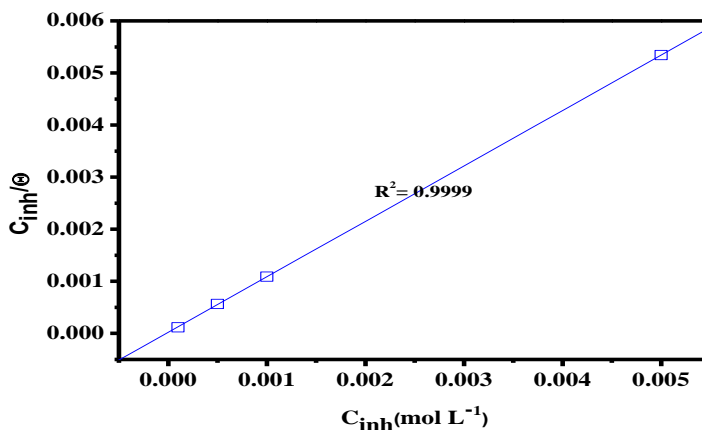


Figure 5. Langmuir adsorption of inhibitor on the MS surface in 1.0 M HCl solution at 303K.

A better straight line is obtained ($R^2 = 0.9999$) with a slope equal ≈ 1.0 . The standard free energy of adsorption, ΔG_{ads}° was determined from the intercept of the plot in Fig. 5. It is found to be $-37.11 \text{ kJ mol}^{-1}$. Normally, the magnitude of ΔG_{ads}° around -20 kJ mol^{-1} or less negative is assumed for electrostatic interactions exist between inhibitor and the charged metal surface (i.e., physisorption). Those around -40 kJ mol^{-1} or more negative are indication of charge sharing or transferring from organic species to the metal surface to form a coordinate type of metal bond (i.e., chemisorption)[15,19]. The above value in this study may suggest physical and chemical adsorption of DPP on the steel surface. In this context, it is believed that in this acid HCl solution, the organic molecules is protonated and DPP molecules acquire positive charge. In the other hand, the adsorption of Cl^- ions on the metal surface turns the surface charge to negative surface, which facilitates the interactions between the positive moieties on the DPP molecules and the negative steel surface.

Monte Carlo simulation

Adsorption of DPP molecules has been studied using Monte Carlo simulation techniques. Adsorption of DPP on iron substrate, Fe (1 1 0) has been studied to find the lowest energy adsorption sites on DPP molecules. The most stable configuration for adsorption of DPP molecules on iron substrate is presented in Figure 6. The outputs and descriptors calculated by the Monte Carlo simulation method are presented in Table 4. Generally, the adsorption energy is defined as most descriptor of the efficiency of an inhibitor. The obtained results show that the DPP associated with high negative values of adsorption energy (-131.05 kcal/mol) resulting in the strong interactions between metal and DPP molecules[29,30]. Which is accordance with the good inhibitive performance of tested compound.

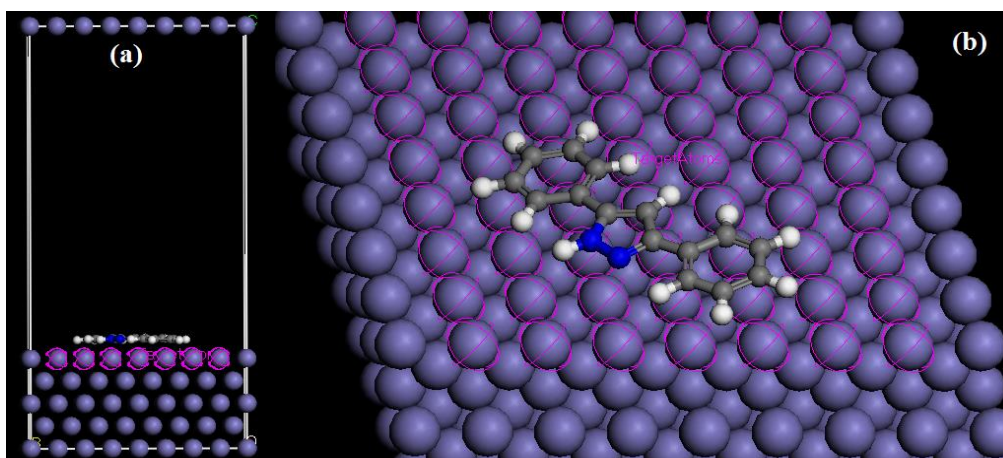


Figure 6. The most stable low energy configuration for the adsorption of the inhibitor on Fe (1 1 0) surface obtained through the Monte Carlo simulation.(a) side view, (b) top view.

Table 4. Outputs and descriptors calculated by the Monte Carlo simulation for the lowest adsorption configurations of DPP Fe (1 1 0) surface (in kcal/mol).

System	Total energy	Adsorption energy	Rigid adsorption energy	Deformation energy	dEad/dNi inhibitor
Fe (1 1 0)/DPP	78.72	-131.05	-130.74	-0.31	-131.05

CONCLUSION

In the present study, it is concluded that the DPP showed excellent inhibition efficiency for mild steel in 1 M HCl. The results obtained from weight loss, electrochemical, and theoretical calculations were in good agreement. The weight loss study showed that inhibition efficiency increases with DPP concentration and maximum values were obtained at 5 mM concentration. Potentiodynamic results suggest that the presence of DPP decreases the rate of anodic mild steel dissolution as well as cathodic hydrogen evolution and act as mixed type inhibitor. The *EIS* results indicate that DPP inhibit mild steel corrosion in 1 M HCl by forming a surface film at metal/electrolyte interfaces. The large negative values of adsorption energy in Monte Carlo simulation indicate the strong interaction between metal and inhibitor.

ACKNOWLEDGEMENTS

Financial support from the Spanish Ministry of Science and Innovation (CTQ2010-61830) is gratefully acknowledged. The support given through a "INCRECYT" research contract to M. Zougagh.

REFERENCES

- [1] Adardour L, Larouj M, Lgaz H, Belkhaouda M, Salghi R, Jodeh S, et al. *Pharma Chem* 2016;8:152–60.
- [2] Adardour L, Lgaz H, Salghi R, Larouj M, Jodeh S, Zougagh M, et al. *Pharm Lett* 2016;8:212–24.
- [3] Adardour L, Lgaz H, Salghi R, Larouj M, Jodeh S, Zougagh M, et al. *Pharm Lett* 2016;8:173–85.
- [4] Adardour L, Lgaz H, Salghi R, Larouj M, Jodeh S, Zougagh M, et al. *Pharm Lett* 2016;8:126–37.
- [5] Afia L, Larouj M, Lgaz H, Salghi R, Jodeh S, Samhan S, et al. *Pharma Chem* 2016;8:22–35.
- [6] Afia L, Larouj M, Salghi R, Jodeh S, Zougagh M, Rasem Hasan A, et al. *Pharma Chem* 2016;8:166–79.
- [7] Bousskri A, Salghi R, Anejjar A, Jodeh S, Quraishi MA, Larouj M, et al. *Pharma Chem* 2016;8:67–83.
- [8] El Makrini B, Larouj M, Lgaz H, Salghi R, Salman A, Belkhaouda M, et al. *Pharma Chem* 2016;8:227–37.
- [9] El Makrini B, Lgaz H, Larouj M, Salghi R, Rasem Hasan A, Belkhaouda M, et al. *Pharma Chem* 2016;8:256–68.
- [10] Larouj M, Belkhaouda M, Lgaz H, Salghi R, Jodeh S, Samhan S, et al. *Pharma Chem* 2016;8:114–33.
- [11] Larouj M, Lgaz H, Salghi R, Jodeh S, Messali M, Zougagh M, et al. *Mor J Chem* 2016;4:567–83.
- [12] Larouj M, Lgaz H, Salghi R, Oudda H, Jodeh S, Chetouani A. *Mor J Chem* 2016;4:425–36.
- [13] Larouj M, Lgaz H, Houda S, Zarrok H, Zarrouk A, Elmidaoui A, et al. *J Mater Environ Sci* 2015;6:3251–67.
- [14] Verma C, Ebenso EE, Bahadur I, Obot IB, Quraishi MA. *J Mol Liq* 2015;212:209–18. doi:10.1016/j.molliq.2015.09.009.
- [15] Verma C, Quraishi MA, Singh A. *J Mol Liq* 2015;212:804–12. doi:10.1016/j.molliq.2015.10.026.
- [16] Yadav M, Kumar S, Sinha RR, Bahadur I, Ebenso EE. *J Mol Liq* 2015;211:135–45. doi:10.1016/j.molliq.2015.06.063.
- [17] Yadav M, Sinha RR, Kumar S, Bahadur I, Ebenso EE. *J Mol Liq* 2015;208:322–32. doi:10.1016/j.molliq.2015.05.005.
- [18] Yadav M, Sinha RR, Sarkar TK, Bahadur I, Ebenso EE. *J Mol Liq* 2015;212:686–98. doi:10.1016/j.molliq.2015.09.047.
- [19] Yadav M, Gope L, Kumari N, Yadav P. *J Mol Liq* 2016;216:78–86. doi:10.1016/j.molliq.2015.12.106.
- [20] Lgaz H, Anejjar A, Salghi R, Jodeh S, Zougagh M, Warad I, et al. *Int J Corros Scale Inhib* 2016;5:209–231.
- [21] Lgaz H, Benali O, Salghi R, Jodeh S, Larouj M, Hamed O, et al. *Pharma Chem* 2016;8:172–90.
- [22] Lgaz H, ELaoufir Y, Ramli Y, Larouj M, Zarrok H, Salghi R, et al. *Pharma Chem* 2015;7:36–45.
- [23] Lgaz H, Salghi R, Larouj M, Elfaydy M, Jodeh S, About H, et al. *Mor J Chem* 2016;4:592–612.
- [24] Lgaz H, Belkhaouda M, Larouj M, Salghi R, Jodeh S, Warad I, et al. *Mor J Chem* 2016;4:101–11.

- [25] Lotfi N, Lgaz H, Belkhaouda M, Larouj M, Salghi R, Jodeh S, et al. Arab J Chem Environ Res 2015;1:13–23.
- [26] Saadouni M, Larouj M, Salghi R, Lgaz H, Jodeh S, Zougagh M, et al. Pharm Lett 2016;8:65–76.
- [27] Saadouni M, Larouj M, Salghi R, Lgaz H, Jodeh S, Zougagh M, et al. Pharm Lett 2016;8:96–107.
- [28] Materials Studio. Revision 6.0. Accelrys Inc., San Diego, USA; 2013.
- [29] Kaya S, Tüzün B, Kaya C, Obot IB. J Taiwan Inst Chem Eng 2016;58:528–35. doi:10.1016/j.jtice.2015.06.009.
- [30] Khaled KF, El-Maghraby A. Arab J Chem 2014;7:319–26. doi:10.1016/j.arabjc.2010.11.005.
- [31] Sasikumar Y, Adekunle AS, Olasunkanmi LO, Bahadur I, Baskar R, Kabanda MM, et al. J Mol Liq 2015;211:105–18. doi:10.1016/j.molliq.2015.06.052.
- [32] Yüce AO, Mert BD, Kardaş G, Yazıcı B. Corros Sci 2014;83:310–6.
- [33] Yadav M, Sinha R, Kumar S, Sarkar T. RSC Adv 2015;5:70832–48.
- [34] Bentiss F, Lebrini M, Lagrenée M. Corros Sci 2005;47:2915–31.
- [35] Verma C, Quraishi MA, Olasunkanmi LO, Ebenso EE. RSC Adv 2015;5:85417–30. doi:10.1039/C5RA16982H.